Strong deviations from Fowler-Nordheim behavior for field emission from individual SiC nanowires due to restricted bulk carrier generation

M. Choueib,[1,2] A. Ayari,[1] P. Vincent,[1] M. Bechelany,[2] D. Cornu,[2] and S. T. Purcell[1,*]
[1]*Université de Lyon, F-69000, France and*
Laboratoire PMCN, CNRS, UMR 5586, Université Lyon 1, F–69622 Villeurbanne Cedex, France
[2]*Laboratoire des Multimatériaux et Interfaces, UMR 5615, CNRS, Université Lyon 1*
and Université de Lyon, 43 Bd du 11 novembre 1918, F-69622, Villeurbanne Cedex, France
(Received 15 July 2008; revised manuscript received 27 November 2008; published 11 February 2009)

We report here field-emission (FE) studies of individual single-crystal SiC nanowires that showed several distinct I/V regimes including strong saturation resulting in highly nonlinear Fowler-Nordheim plots. The saturation is due to the formation of a depletion layer near the nanowire ends as predicted for FE from semiconductors and appears after *in situ* control of the surface cleanliness. This work opens the door to improving the uniformity, stability, and photon control of mass-produced planar nanowire FE cathodes and shows how FE can be used for transport measurements on individual semiconducting nanowires.

DOI: 10.1103/PhysRevB.79.075421 PACS number(s): 79.70.+q, 73.63.−b, 61.46.−w

I. INTRODUCTION

Field emission (FE) from carbon nanotubes[1] (CNTs) has attracted appreciable interest for both applications and the fundamental physics of quasi-one-dimensional objects. There are several important advantages of CNTs as field emitters such as high-field amplification, mass fabrication, current stability, high current carrying capability, and robustness. As a result numerous large and medium scale applications have been identified:[2] flat panel displays, lighting, portable x-ray generators, rf amplifiers, etc. On the fundamental side, it has been shown that FE can also access simultaneously electrical, thermal, optical, and mechanical properties[3–5] of an individual CNT. In contrast to CNTs, there has been much less work on FE from another important quasi-one-dimensional system, semiconducting nanowires (NWs), even though they are now a distinct and large research domain.[6,7] They can also be produced with the same geometries as CNTs on either tip or planar surfaces, amenable to similar applications. An important difference is that the more predictable band gaps and doping methods of semiconducting NWs open different possibilities compared to CNTs, which have been of the metallic type in all FE experiments on these $1d$ emitters.

In view of this there is a clear need for in-depth studies of FE from individual NWs: first for the different opportunities that NWs may create for FE cathodes and second for the possibility of using FE to measure different properties of NWs. This last should be useful for meeting two of the major challenges facing the NW research community. (1) What is the role of the surface in different physical processes, such as electronic transport and optical absorption, in these objects of large surface-to-volume ratio[8] and (2) how can the doping be controlled or even measured when unwanted impurities and surface segregation[9] are common phenomena. Though certain groups have achieved p- and n-type dopings and their characterization by integrating them into transistor structures,[10] such control and analysis has only been applied to a small minority of the many synthesis methods now being developed.

The emitted current density J from metallic or semimetallic emitter through the triangular surface tunneling barrier is governed by the famous Fowler-Nordheim (FN) theory.[11] The FN equation is $J=A(\beta V)^2\exp(-\frac{B\phi^{3/2}}{\beta V})$, where A and B are roughly constant, ϕ is the work function ($\sim$5 eV), and $F=\beta V$ is the applied field with β the geometrical factor at the emitter surface and V is the applied voltage. Emission is dominated by the exponential term that comes from the tunneling probability. There is only a modest correction for temperature. Plotting $\log(\frac{I}{V^2})$ vs $\frac{1}{V}$ (the FN plot) should give a straight line and this has been verified literally thousands of times since the first report of Millikan and co-workers.[12] Most measurements on CNTs follow quite well this equation though more or less strong deviations can occur due to a host of nonintrinsic effects such as a resistance drop along the CNT,[13] high temperatures due to Joule heating,[3] adsorption-desorption cycles,[14] space charge,[15] etc.

Though much less extensive than the work on metals, there has been significant theoretical and experimental work done on FE from semiconductors from the 1960s until now. The specific cases of p-type doping and high-resistivity n-type samples are interesting because they can lead to very dramatic nonlinear FN plots. I/V characteristics are divided into three different emission regimes (I–III) (see inset of Fig. 1) as the current follows or deviates with respect to standard FN theory. The regimes are predicted by theory[16] and have been verified in experiment[17–20] for properly prepared macroscopic FE tips. In particular for the p-type case (see Fig. 1), a space-charge region can form within the emitter tip near the apex because field emission takes place from the degenerated conduction band where the height of the tunnel barrier is smaller, whereas most of the bulk carriers are in the valence band.

The three regimes are distinguished as follows (going from low to high currents): (i) Region I: standard FN or zero current approximation. The number of electrons at the emission zone is sufficient and $J(V)$ is determined only by the tunneling probability. The conduction band is strongly degenerated at the apex due to field penetration and behaves similar to a metallic emitter. (ii) Region II: saturation. Emission is limited by insufficient carrier supply through the gap. This regime is often assimilated to a p-n junction in reverse

1098-0121/2009/79(7)/075421(7)

©2009 The American Physical Society

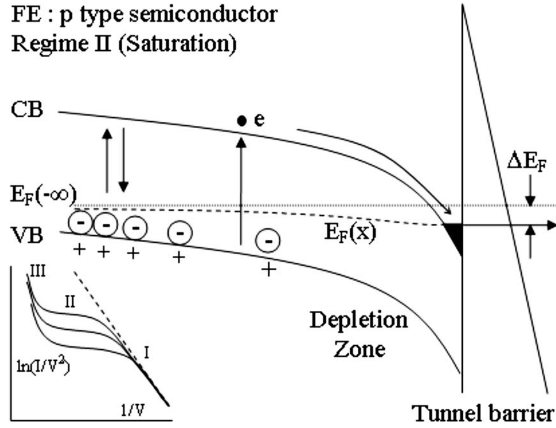

FIG. 1. Potential-energy diagram in the near surface region for field emission from a p-type semiconductor in regime I. A space-charge region builds up behind a pocket of electrons formed in the degenerate conduction band. Emission occurs below the bulk Fermi level by an amount ΔE_F directly measurable with the energy analyzer. Inset: schematic of the theoretical Fowler-Nordheim plots depicting the three current regimes and the effects of temperature or light.

bias. In contrast to standard FN emission, the current is strongly dependent on temperature and light because the generation of free carriers affects the depletion zone. (iii) Region III: rapid increase. The field penetration is sufficient for impact ionization in the space-charge region and carrier density progressively increases. This regime is less studied and other mechanisms may play an important role such as Zener tunneling. In the highly resistive n-type case, the saturation regime is similar in that it is characterized by a too low total current with some region of high drift and diffusion currents. However, the role played by the energy gap is now played by the dopant ionization energy. The saturation in region II is the most interesting for applications because the emission current is bulk controlled and much less sensitive to the surface of the apex. This aids in current stability, uniformity of emission from emitters of different β, and control of emission by temperature and light; this last opens up applications for photocathodes. Successful observation of these regimes even for macroscopic tips is very dependent on sample preparation and is often completely masked by unwanted surface short circuiting due to adsorption, surface segregation, defects, etc.[21] This is exacerbated for NWs because of the high surface-to-volume ratio. Consequently region II is easily hidden by surface leakage which is likely why it has not yet been observed for NWs. The effect on the FN plots is described in Fig. 2 which shows that the temperature dependence is reduced as the emission process approaches FN theory.

The few measurements in the literature on NWs have only shown standard FN behavior whether for multiple emitters dispersed over planar supports[22–25] or for individual NWs grown or mounted on support tips.[26,27] In this paper, we report I/V and FE electron spectra (FEES) studies of several individual SiC nanowires as a function of temperature. The nanowires were submitted to *in situ* temperature and ion bombardment cycles. Properly prepared nanowires showed

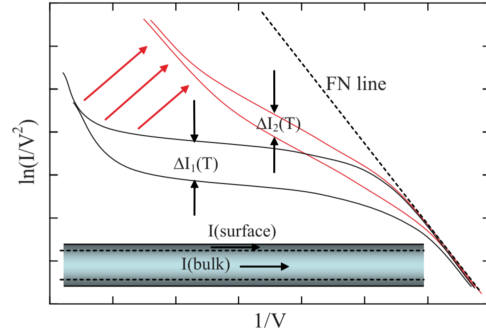

FIG. 2. (Color online) Schematic Fowler-Nordheim plots for a nanowire with different modes of transport, for example, through surface layers or by defects or a range of deep dopants. As more conduction channels are available, the curves will evolve toward a standard FN plot reducing the effects of temperature and light.

strongly nonlinear FN plots with the three regimes that are predicted by the FE theory for semiconductors. That is, the nonlinearity is not due to obvious secondary effects but to insufficient carrier supply from within the NW itself. The emission was strongly dependent on temperature.

The paper is organized as follows. Section II describes our experimental setup. The experimental results are shown in Sec. III, and Sec. IV is dedicated to the interpretation of our results. A brief conclusion is given at the end of this paper.

II. EXPERIMENT

We have carried out FE studies of individual wide band gap SiC NWs synthesized in mass at high temperature by a pure vapor solid process[28] that uses no catalyst. These NWs have been extensively studied by our groups over the last few years by FE, scanning electron microscopy (SEM), transmission electron microscopy[28] (TEM), and Raman spectroscopy[29] and have been used as cantilevers in mechanical resonance experiments.[30–32] In particular TEM studies showed that the NWs were single-crystalline 3C-SiC with various concentrations of stacking faults and covered by a native oxide layer of several nanometers. The stacking faults, which can be seen as inclusions of other polytypes into 3C-SiC, can lead to variable band gaps along the nanowire.

Individual NWs of different diameters (35–200 nm) were attached by conductive carbon glue to the ends of tungsten tips obtained by electrochemical etching [Fig. 3(a)]. The attachment of NWs having diameters greater than 75 nm was done using a micromanipulator and an optical microscope. NWs with small diameters were mounted with a three-dimensional nanomanipulator in a SEM.[33]

All FE measurements, such as the dependence of emitted current I_{FE} on time, voltage, and temperature, FE microscopy (FEM) imaging, and FE electron spectroscopy (FEES) of the total-energy distributions (TEDs) of the emitted electrons, were performed in an ultrahigh vacuum (UHV) system at a pressure of 2×10^{-10} Torr. The W tip was held in a 1-mm-diameter nickel tube spot welded to a tantalum loop to allow *in situ* cleaning by standard Joule heating. The experimental

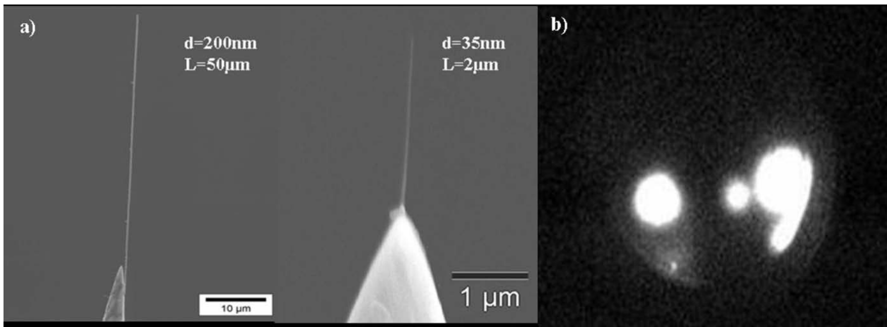

FIG. 3. (a) SEM images of two nanowires NW1 (diameter d $=200$ nm and length $L=50$ μm) and NW2 ($d=35$ nm, L $=2$ μm) mounted on a tungsten tip. (b) Field-emission patterns of the NW2 show several bright spots due to localized emission from higher radius of curvature zones.

setup for the field-emission measurements has been reported in detail elsewhere[3] and reduced to its minimum consists of a negatively polarized emitter facing a phosphor screen several centimeters away on which the FE pattern is formed by the projected emitting electrons. The emitter head can also be reoriented so that the electrons enter into an energy analyzer which allows a direct measurement of the voltage drops (or electrical resistances) along the nanowire or an electron counter for very low current measurements (see below). The temperature could be varied between 80 K and typically 1200 K. The NW temperature (T) versus the current in the heating loop was determined by a chromel-alumel thermocouple spot welded onto the nickel tube and micropyrometer measurements for T above 700 °C. The system had a home-built ion bombardment system which allowed uniform bombardment by different gas ions down to 50 eV.

Two particular difficulties were encountered throughout these experiments. First FEM and FEES were often difficult because the NWs tend to break off along transverse cleavage planes from the much longer wires produced during growth. This often gave apex edge emission off the NW axis that was difficult to align with the energy analyzer and even the FEM screen. As of the present, our better FEM patterns consisted of random spots due to fairly localized emission zones [Fig. 3(b)] without the possibility of distinguishing the apex crystallography. Field ion evaporation at high reverse fields on this covalent material usually could not round and smooth the NW ends and sometimes the whole NW was removed from the W support tip. Second, the SiC nanowires can undergo sudden transformations during FE generally at higher currents and temperature where, for example, the electrical resistivity is decreased by a factor of 100, thus exhibiting metallic behavior. These difficulties mean that one NW could not yet be taken through all the types of measurements and thus partial and overlapping results of different NWs will be exposed to demonstrate the experiments.

III. RESULTS

Measurements on several SiC NWs of different diameters (35–175–200–250 nm) were carried out. Figure 3 shows two NWs denoted NW1 (diameter $d=200$ nm; length L $=50$ μm) and NW2 ($d=35$ nm, $L=2$ μm). The measured NWs ($d=175$ nm, $L=65$ μm) and (d $=250$ nm, $L=55 \mu$m) are denoted NW3 and NW4, respectively.

Prior to FE measurements, the NWs were precleaned to 800 K in UHV for 2 min to desorb the volatile layers that are always present on surfaces exposed to air. The FE current was then extremely stable (Fig. 4). In fact the stability is as good as carbon nanotubes in similar vacuum,[5] though at first with lower sustainable currents (see below). Thus despite the quite large band gap of 2.4 eV, SiC NWs without intentional doping can be used as field emitters. The intrinsic carrier density would only be $10^{-2}/\text{cm}^3$ at room temperature convertible into a resistance of 10^{23} Ω for a reasonable carrier mobility of 380 $\text{cm}^2/\text{V s}$ and the dimensions of NW1. The question then is: what is the transport mechanism? For example, typical accidental n-type doping by N in bulk crystals of $10^{17}-10^{18}/\text{cm}^3$ is common. The level and type of accidental doping is not known *a priori* for this growth method and conduction through a surface layer is very possible (even likely) in these small structures.

First current-voltage (I-V) measurements often showed what appeared at first glance to be metal-like emission, i.e., linear FN plots, but they were very sensitive to temperature (T) and the slopes of the FN plots were much lower than can be explained with theory unless a ridiculously low ϕ is invoked. This sensitivity to T is not in agreement with metallic emission but is for semiconductors where the density of carriers is thermally activated especially for deep donors or large gap semiconductors. However, the three predicted regimes were not distinguishable.

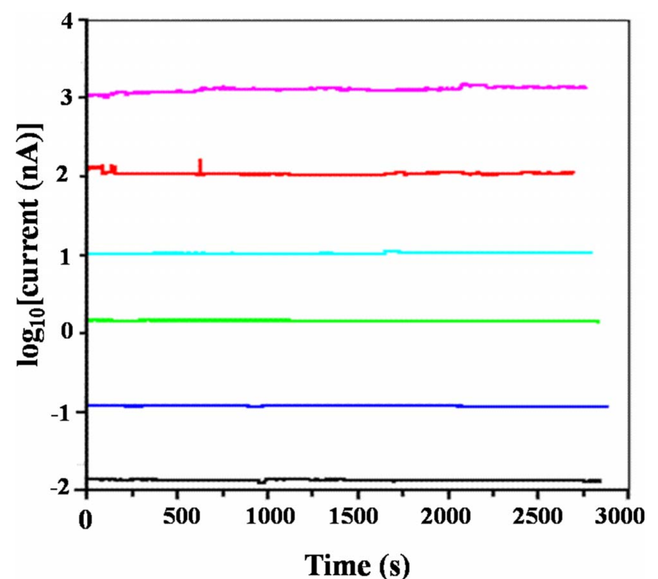

FIG. 4. (Color online) Emission current stability of NW3 for different voltages at room temperature.

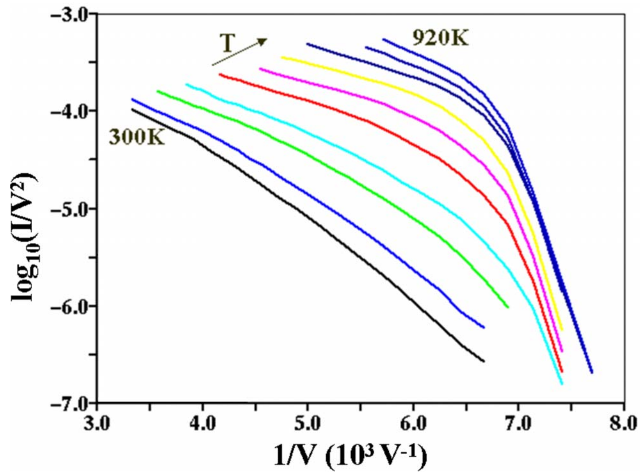

FIG. 5. (Color online) FN plots for NW1 after Ar ion bombardment and with increasing temperature with steps of 70 K from room temperature up to 920 K for the NW1 showing high sensitivity to temperature. At high temperature, there are clearly two regions (I and II in inset).

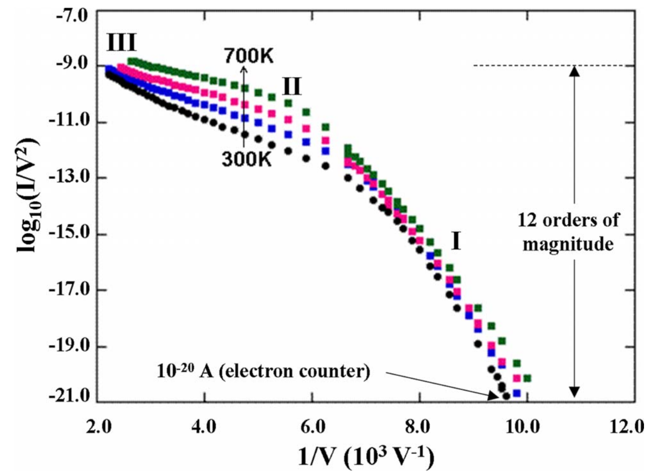

FIG. 6. (Color online) FN plots for NW4 with increasing temperature. One distinguishes the three regions: region I appears at a very low current ($10^{-21}-10^{-14}$ A) measured with the single electron counter; region II is very sensitive to temperature; and we can notice the beginning of region III.

We then performed ion bombardment to remove the surface layer and perhaps the native oxide on the NWs. Low-energy ion sputtering at room temperature with Ar (50–100 eV) at a feed pressure of 1×10^{-4} Torr and subsequent annealing resulted in essential modifications in the *I*-*V* curves. Ion penetration distances at these energies are in the 1 nm range and thus this is essentially surface erosion. In Fig. 5 we present FN plots with increasing temperature up to 920 K for the NW1. The curves are strongly nonlinear, particularly at high temperature where the regimes I and II are clearly distinguished. Emission is highly sensitive to T with a maximum of $[\mathrm{I}(920)\text{-}\mathrm{I}(300)]/\mathrm{I}(300)\sim300$. At lower temperatures, one observes only a linear curve which we still ascribe to regime II. We would need to measure currents well below 10^{-13} A to observe regime I in this case (see below). Regime III was not observed here because we limited the emission current to approximately 10 nA, in order not to damage the nanowire and prevent current hysteresis from charge trap motion under a high electric field. The saturation behavior was reproduced for all four NWs.

To decrease the minimal detectable current, we placed a single electron counter in the system. This permits us to measure currents to very low levels. A background noise level of still undetermined origin has limited us at present to 10^{-21} A with saturation at approximately 10^{-13} A, which just overlaps our electrometer. Another series of FN plots is shown in Fig. 6 which now shows the FN behavior well followed for the regime I branch which could, in principle, now be used to estimate the electron affinity. Such low currents are seldom if ever explored in FE. An interesting feature is that on descending the branch I, the current becomes more and more sensitive to temperature after a minimum sensitivity at the meeting point of regimes I and II. This is a consequence—or if one prefers a confirmation—of the applicability of FN theory here because the coefficient multiplying the T^2 correction increases on reducing the field.[34]

To observe regime III a higher internal electric field is needed. To do so for the same range of current, we attempted to decrease the number of carriers. Several bombardment cycles with argon and FE desorption shortening were carried out in order to reduce even further surface leakage. A series of I/V curves is shown in Fig. 7 that now clearly shows the transition from regime II to regime III. Regime I is barely visible at 865 K. As previously reported[3] the position of the TEDs gives the voltage drops along the NW and plotting the emitted current against their position is equivalent to a two point transport measurement with one bias direction available. In Fig. 8, we present the plot of emitted current versus voltage drop along the nanowire corresponding to the FN plots of Fig. 6. The voltage drops are quite large reaching 150 V. On log scale for I, these curves have two slopes which

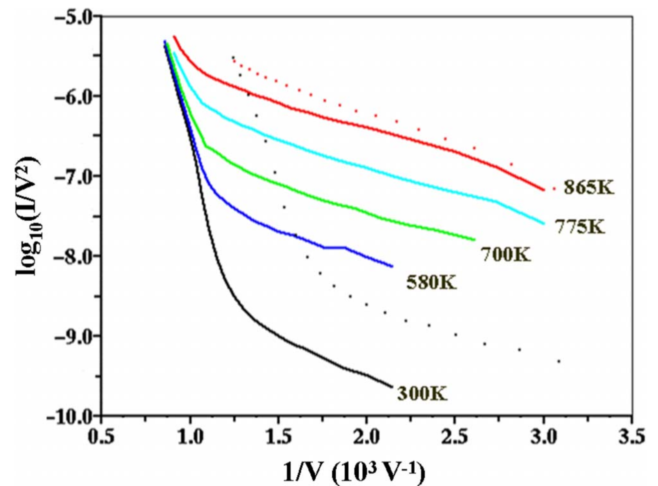

FIG. 7. (Color online) FN plots after several argon-ion bombardment cycles and FE desorption shortening for NW1 at different temperatures. These curves show two regions (II and III) where only the region II is sensitive to temperature. At 775 and 865 K, we can hardly distinguish region I. The dotted lines (black at 300 K and red at 865 K) correspond to a correction for the voltage drop measured in Fig. 8 (see Discussion).

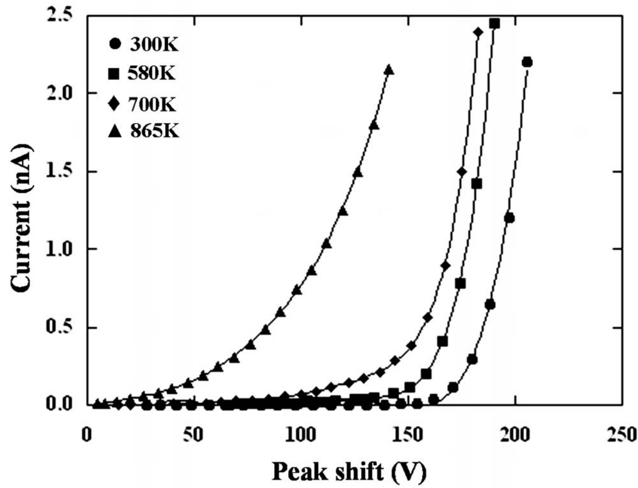

FIG. 8. Emission current versus tip voltage drop for NW1 at different temperatures corresponding to the FN plots of Fig. 7.

correspond to the two regimes II and III of Fig. 7. The exponential behavior in regime II indicates a non-ohmic behavior, the origin of which (bulk or contact) will be discussed in the next paragraph.

All the measurements presented above were reproducible over the measurement cycles; however, for high-temperature treatments ($T>1000$ K) the nonlinearity in the FN curves could suddenly disappear accompanied by transformations to lower resistance. The FN plot followed the schematic of Fig. 2. This irreversible effect was also observed for bulk semiconductor emitters by Arthur[17] and Fursey[18] when the emitter was heated to 450 K in vacuum. According to these authors, this effect is attributed to the formation of a conducting skin along the emitter. In our case, the conduction skin is likely due to the segregation of carbon at the surface and the preferential volatility of silicon in the temperature range of 1300–1450 K.[35] The saturation effects could often be recuperated by new bombardment cycles which is strong proof that the modifications are due to surface changes. It is worth noting that the transformed nanowires can emit stable currents up to 10 μA, approaching values for carbon nanotubes ostensibly due to reduced heating effects. This is much higher than previously reported for individual nanowires[26,27] and is useful for high current applications, though the emission is then no longer sensitive to temperature or light.

IV. DISCUSSION

The FE clearly follows the broad lines predicted by semiconductor theory with the three regimes distinguished when the NW surface is properly prepared. We have carried out some analysis of this system with the goal of quantifying this agreement; but as we discuss below a close correlation with experiments is presently not possible. The bulk or surface doping of these NWs is not known *a priori* though Raman studies have recently given evidence for room-temperature carrier densities in the $10^{18}-10^{19}$ cm^{-3} range for pristine NWs fabricated by this procedure.[29]

For untreated NWs, we simply propose that the carriers come mainly from the residual amorphous SiO_x layer at the surface as the saturation is visible only after ion bombardment which removes most of this layer. For the treated nanowires, a simple explanation of the saturation current due to a highly resistive Ohmic nanowire does not work. The strong bending of the Fowler-Nordheim curves cannot be explained just by an additional voltage drop along the nanowire. This can be seen in Fig. 7 where we made the correction for the voltage drop measured with the TEDs in Fig. 8. A shift of the curve is obtained but not a change in its form or slope. The exponential behavior of the current in Fig. 8 could also be interpreted as coming from a Schottky barrier at the contact between the tip and the nanowire. However, a 100 V voltage drop across such a barrier for a single nanowire is enough to reduce its thickness to the point where it conducts current such as an ohmic contact. So, carrier-concentration effects must be taken into account.

The activation energy E_A of the saturation current can give insight into the doping of the semiconductor. For a p-type semiconductor emitter, the saturation current is attributed to thermally generated electrons and holes over the diffusion region and is proportional to n_i^2 the intrinsic carrier density as in a classical p-n junction in reverse bias. A more refined model for the p-n junction also involves carriers coming from recombination in the depletion region and surface recombination to explain some of the discrepancy between predicted and measured saturation current. However, these two additional currents are proportional to n_i. The two mechanisms are experimentally distinguishable because the activation energy will be $E_{gap}/2$ for n_i^2 and E_{gap} for n_i-type carrier generation, respectively. An even further refined model,[20] including the effect of trap charges, gives a more complicated activation energy that depends on $E_{gap}/4$ for a specific geometry of the emitter. For an n-type semiconductor, the saturation current is due to thermally generated electrons from the dopant to the conduction band. From elementary semiconductor theory,[36] the activation energy is E_d (the dopant energy ionization) at low temperature, $\frac{1}{2}E_d$ at intermediate temperature, and zero when all the dopants are ionized. The gap for our cubic SiC is 2.4 eV (Ref. 37) and from the experimental growth conditions, the possible accidental dopants during synthesis are N [n type $E_d \sim 0.1$ eV (Ref. 37)] and Al (p type). We observed two regimes in activation energy with a crossover at ~ 600 K. The low temperature E_A is between 0.3 eV (for NW3) and 0.125 eV (for NW2) with a fairly linear $1/T$ dependence of the logarithm of the current. Such an activation energy could be in agreement with an N doping; however, its variability for different samples is more in favor of a contribution from a remaining disordered SiO_x layer. The high-temperature data for NW1 give a fitted E_A of 0.8 eV [see Fig. 9(a)] which decreases with increasing voltage. This value clearly rejects a purely p-type scenario and indicates that traps should play an important role. This conclusion is supported by the field dependence of E_A as expected for a Poole-Frenkel mechanism[38] and by the increasing current as a function of voltage in regime II instead of nearly perfect saturation. Varying slopes in regime II have also been observed by others[19,20] and are attributed to the weight of additional transport mechanisms, especially the

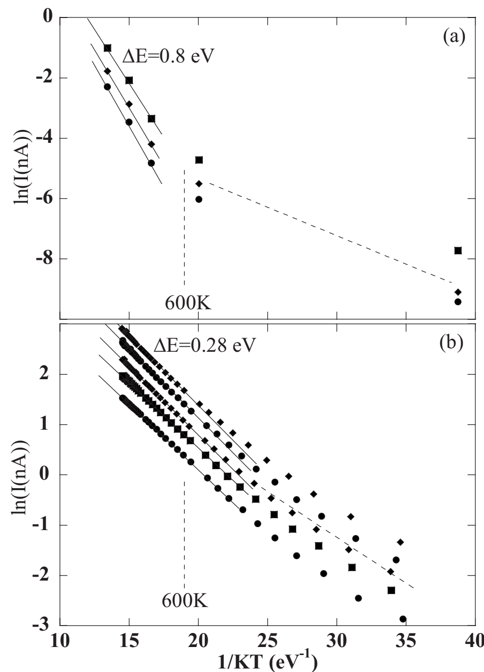

FIG. 9. (a) Arrhenius plots of the emission current for NW1 at three different voltages taken from Fig. 6 [(●) at 500 V with an activation energy of 0.80 eV, ▲ at 566 V with an activation energy of 0.76 eV, and (■) at 666 V with an activation energy of 0.74 eV]. (b) Arrhenius plots for NW4 corresponding to its state for which the FN plots of Fig. 6 were measured.

Poole-Frenkel effect. The difference in E_A between the low-temperature and high-temperature regimes explains why even in an insufficiently cleaned sample as in Fig. 4, the saturation tends to be visible at 900 K, since the *p*-type trap-assisted current dominates at high temperature. A frequent complication should be mentioned; that is, the fitting to $I(T)$ curves for samples with weak saturation due to the existence of surface conduction leads to reduced values of E_A as explained in Fig. 2. An example is shown in Fig. 9(b) corresponding to the FN plots of Fig. 6 which gave a low E_A of 0.275 eV. A final remark is that we believe that the saturation effects are well observed here at high temperatures, in contrast to previous work on other emitters because of the larger band gap of SiC.

V. CONCLUSION

In this study, we have succeeded in modifying *in situ* the surface of mass-produced nanowires by ion bombardment, thus revealing a saturation phenomenon previously observed only in bulk emitters. These are accompanied by a high sensitivity of emission to temperature. Analysis of the data gives evidence of the *p*-type doping with trap-assisted transport at temperature above 700 K. It is only the combination of variable-temperature FEES and Fowler-Nordheim measurements that allowed us to determine the transport mechanism involved in these nanowires with *a priori* unknown conducting characteristics. We anticipate that this work opens a rather wide range of perspectives for semiconducting nanowire field emitters ranging from theory and basic research to applications. Hand in hand with the temperature dependence, we have already demonstrated a high sensitivity of the emission to laser light which we will expose in a future publication. This opens a different route to highly efficient planar photocathodes. The high current carrying possibility of transformed nanowires can address high current applications at present explored with carbon nanotubes. The complexity and uncertainty of the initial conduction state of these nanowires means that only general conclusions could be made at this time; however, it appears that the original theory provides a proper basis for analysis. Studies on nanowires with identified doping are now obviously imperative. Mastering this is also a prerequisite for understanding emission from even thinner nanowires—say below 20 nm—where confinement effects exist.

ACKNOWLEDGMENTS

This work was carried out within the framework of the Group Nanowires-Nanotubes Lyonnais. M.C. thanks the Lebanese CNRS for financial support.

*stephen.purcell@lpmcn.univ-lyon1.fr

[1] See, for example, W. De Heer, A. Châtelain, and D. Ugarte, Science **270**, 1179 (1995).
[2] N. De Jonge and J.-M. Bonard, Philos. Trans. R. Soc. London, Ser. A **362**, 2239 (2004).
[3] S. T. Purcell, P. Vincent, C. Journet, and V. Thien Binh, Phys. Rev. Lett. **88**, 105502 (2002).
[4] S. T. Purcell, P. Vincent, C. Journet, and V. T. Binh, Phys. Rev. Lett. **89**, 276103 (2002).
[5] S. T. Purcell, P. Vincent, M. Rodriguez, C. Journet, S. Vignoli, D. Guillot, and A. Ayari, Chem. Vap. Deposition **12**, 331 (2006).
[6] W. Lu and C. M. Lieber, J. Phys. D **39**, R387 (2006).
[7] P. Yang, MRS Bull. **30**, 85 (2005).
[8] M. V. Fernandez-Serra, C. Adessi, and X. Blase, Nano Lett. **6**, 2674 (2006).
[9] M. V. Fernandez-Serra, C. Adessi, and X. Blase, Phys. Rev. Lett. **96**, 166805 (2006).
[10] G. Zheng, W. Lu, S. Jin, and C. M. Lieber, Adv. Mater. (Weinheim, Ger.) **16**, 1890 (2004).
[11] R. H. Fowler and L. W. Nordheim, Proc. R. Soc. London, Ser. A **119**, 173 (1928).
[12] C. F. Eyring, S. S. Mackeown, and R. A. Millikan, Phys. Rev. **31**, 900 (1928).
[13] E. Minoux, O. Groening, K. B. K. Teo, S. H. Dalal, L. Gangloff, J. P. Schnell, L. Hudanski, I. Y. Y. Bu, P. Vincent, P. Legagneux, G. A. J. Amaratunga, and W. I. Milne, Nano Lett. **5**, 2135 (2005).
[14] K. A. Dean, Appl. Phys. Lett. **76**, 375 (2000).

[15] N. S. Xu, Y. Chen, S. Z. Deng, J. Chen, X. C. Ma, and E. G. Wang, Chin. Phys. Lett. **18**, 1278 (2001).
[16] L. M. Baskin, O. I. Lvov, and G. N. Fursey, Phys. Status Solidi B **47**, 49 (1971).
[17] J. R. Arthur, J. Appl. Phys. **36**, 3221 (1965).
[18] G. N. Fursey and N. V. Egorov, Solid State Phys. **32**, 23 (1969).
[19] D. K. Schroder, R. N. Thomas, J. Vine, and H. C. Nathanson, IEEE Trans. Electron Devices **21**, 785 (1974).
[20] K. X. Liu, C. J. Chiang, and J. P. Heritage, J. Appl. Phys. **99**, 034502 (2006).
[21] G. N. Fursey, *Field Emission in Vacuum Microelctronics* (Academic, New York, 2005).
[22] Z. S. Wu, S. Z. Deng, N. S. Xu, Jian Chen, J. Zhou, and Jun Chen, Appl. Phys. Lett. **80**, 3829 (2002).
[23] B. Zeng, G. Xiong, S. Chen, S. H. Jo, W. Z. Wang, D. Z. Wang, and Z. F. Ren, Appl. Phys. Lett. **88**, 213108 (2006).
[24] D. Banerjee, S. H. Jo, and Z. F. Ren, Adv. Mater. (Weinheim, Ger.) **16**, 2028 (2004).
[25] Y. W. Zhu, T. Yu, F. C. Cheong, X. J. Xu, C. T. Lim, V. B. C. Tan, J. T. L. Thong, and C. H. Sow, Nanotechnology **16**, 88 (2005).
[26] C. H. Jin, Z. Y. Zhang, J. Y. Wang, Q. Chen, and L.-M. Peng, Appl. Phys. Lett. **89**, 213108 (2006).
[27] E. C. Heeres, E. P. A. M. Bakkers, A. L. Roest, M. Kaiser, T. H. Oosterkamp, and N. De Jonge, Nano Lett. **7**, 536 (2007).
[28] M. Bechelany, A. Brioude, P. Stadelmann, G. Ferro, D. Cornu, and P. Miele, Adv. Funct. Mater. **17**, 3251 (2007).
[29] M. Bechelany, A. Brioude, D. Cornu, G. Ferro, and P. Miele, Adv. Funct. Mater. **17**, 939 (2007).
[30] S. Perisanu, P. Vincent, A. Ayari, M. Choueib, M. Bechelany, D. Cornu, and S. T. Purcell, Appl. Phys. Lett. **90**, 043113 (2007).
[31] A. Ayari, P. Vincent, S. Perisanu, M. Choueib, V. Gouttenoire, M. Bechelany, D. Cornu, and S. T. Purcell, Nano Lett. **7**, 2252 (2007).
[32] P. Vincent, S. Perisanu, A. Ayari, M. Choueib, V. Gouttenoire, M. Bechelany, A. Brioude, D. Cornu, and S. T. Purcell, Phys. Rev. B **76**, 085435 (2007).
[33] N. De Jonge, Y. Lamy, K. Schoots, and T. H. Oosterkamp, Nature (London) **420**, 393 (2002).
[34] See, for example, L. W. Swanson and A. E. Bell, in *Adv. in Electronics and Electron Phys*, edited by L. Marton (Academic, New York, 1973), Vol. 32, p. 193.
[35] M. J. Bozack, Phys. Status Solidi B **202**, 549 (1997).
[36] N. W. Ashcroff and N. D. Mermin, *Solid State Physics* (Saunders College, Fort Worth, TX, 1976).
[37] G. L. Harris, *Properties of Silicon Carbide* (INSPEC, London, 1995).
[38] J. R. Yeargan and H. L. Taylor, J. Appl. Phys. **39**, 5600 (1968).